

J. Grohmann, B. Rauch, T. Kathrotia, W. Meier, M. Aigner, Influence of single-component fuels on gas turbine model combustor lean blowout, Journal of Propulsion and Power 34 (2018) 97-107.

The AIAA version of the paper is accessible at
<http://dx.doi.org/10.2514/1.B36456/>

On the AIAA web page
<http://www.aiaa.org/content.cfm?pageid=2>
the interested reader can find other material published by AIAA

Influence of single-component fuels on gas turbine model combustor lean blowout

J. Grohmann^a, B. Rauch^b, T. Kathrotia^c, W. Meier^d and M. Aigner^e
German Aerospace Center (DLR), Institute of Combustion Technology,

Pfaffenwaldring 38-40, 70569 Stuttgart, Germany

The influence of selected single-component hydrocarbons on lean blowout behavior of swirl-stabilized spray flames was investigated. Additional information on the spray characteristics was collected by Phase Doppler Interferometry (PDI) and Mie scattering measurements. The measurements were accomplished in a gas turbine model combustor under atmospheric pressure and at two different air preheat temperatures. The combustor featured a dual-swirl geometry and a prefilming airblast atomizer. The combustion chamber provided good optical access and yielded well-defined boundary conditions. Three single-component hydrocarbons were chosen: one short and one long linear alkane (*n*-hexane and *n*-dodecane) and one branched alkane (*iso*-octane). Kerosene Jet A-1 was used as a reference. Results show noticeable differences in the lean blowout limits of the various fuels, at comparable flow conditions. By using the results of the measurements, of additional modelling and of an assessment of the fuel properties it was concluded that fuel differences in lean blowout in this combustor can be due to differences in the physical properties as well as in the chemical properties.

^a Research Associate, DLR, Institute of Combustion Technology, Stuttgart, Germany

^b Research Associate, DLR, Institute of Combustion Technology, Stuttgart, Germany

^c Post-Doctorate, DLR, Institute of Combustion Technology, Stuttgart, Germany

^d Senior Scientist, DLR, Institute of Combustion Technology, Stuttgart, Germany

^e Professor, DLR, Director of the Institute of Combustion Technology, Stuttgart, Germany

Nomenclature

d_0	= initial drop diameter (m)
d_{32}	= Sauter mean diameter (m)
d_i	= prefilmer diameter (m)
λ_{eff}	= effective evaporation rate (m^2/s)
μ	= dynamic viscosity ($\text{Pa}\cdot\text{s}$)
n	= refractive index (-)
\dot{m}	= mass flow rate (kg/s)
ϕ	= global equivalence ratio (-)
P_{th}	= thermal power (W)
ρ	= density (kg/m^3)
Re	= Reynolds number (-)
σ	= surface tension (N/m)
S	= geometrical swirl number (-)
t_e	= total evaporation time (s)
T	= temperature (K)
u, v, w	= velocities in reference coordinate system (m/s)
x, y, z	= reference coordinate system (m)

I. Introduction

Production pathways for alternative aviation fuels offer the possibility to modify the chemical composition of the final product in order to improve physical and chemical properties for optimized combustion performance. Depending on feedstock (e.g. coal, natural gas or biomass) and process parameters, alternative fuels can contain hydrocarbons of significantly different types and chain lengths [1, 2]. However, the influence of the chemical composition of the fuel on combustion performance is not fully understood [3].

Four main processes govern the combustion of liquid fuels in gas turbine combustors: atomization, vaporization, turbulent mixing and chemical reaction. These processes happen simultane-

ously, have strong interactions and cannot be easily independently measured inside the combustor. They depend on different physical and chemical properties, show variable dependence on operating conditions, such as temperature, pressure, flow field and boundary conditions and vary with fuel composition. Because of this, a fuel variation is always a multi-parameter variation (e.g. in viscosity, boiling point and ignition delay time). For the design of fuels or fuel optimized combustors it is necessary to know whether the fuel properties that are related to a certain subprocess are at all relevant. Therefore it is important to be able to estimate the influence of certain fuel properties on a chosen combustion performance criterion (e.g. lean blowout). Particularly, the relative influence of a subprocess (relative compared to the influence of the other subprocesses) is of interest. This is a great challenge that needs input from experimental, theoretical and numerical studies.

For this study a recently developed gas turbine model combustor was used to experimentally investigate the influence of fuel variation on the lean blowout (LBO) behavior. Boundary conditions, such as air, fuel and wall temperatures, were well defined and measured in detail, as the collected data are also used for CFD validation. The combustor setup exhibits characteristics of real aero-engines, i.e. airblast atomization of liquid fuel and a turbulent swirling flow field in a confined combustor. Having these features will complicate interpretation of the results because of the above mentioned overlap of the various processes. It is, however, a necessary step in understanding fuel influence on lean blowout since the interaction between the processes cannot be captured by individual experiments for those processes. The experiments described in this work have been performed at atmospheric pressure. More details on the combustor and the experimental setup can be found in a previous publication [4], as well as its flow field, liquid fuel loading and flame luminosity.

To reduce the additional complexity of the physical and chemical processes of multi-component fuels, single-component fuels have been used. Our goal is to gain a fundamental understanding of the influence of these fuels on a typical gas turbine combustion system, before working on fuel mixtures or even fuel optimization. Hence, experiments were performed with three fuels from the chemical classes of normal and branched hydrocarbons (*n*-hexane, *n*-dodecane and *iso*-octane). For comparison kerosene Jet A-1 was used as a reference. The three single component fuels have been selected because of their physical and chemical properties. They represent typical components of

conventional and alternative jet fuels. By taking advantage of similarities and differences in certain physical and chemical properties of the selected fuels we specifically aim to understand fuel related differences in lean blowout behavior (in contrast to the lean blowout process itself). To support the analysis, information from vaporization modelling and chemical kinetics modelling were used.

II. Lean blowout and fuel influence

In the past, various aspects of spray combustion were studied using laboratory scale model combustors with prefilming airblast atomizers, more or less similar to the one used in this study [5–12]. The majority of the investigations used kerosene or a kerosene surrogate as a fuel. To the authors’ knowledge, the influence of different single component hydrocarbon fuels on airblast atomized swirling spray flames, has not been investigated in detail. This study investigates fuel influence on lean blowout behavior of airblast atomized swirling spray flames. There is general interest in understanding lean blowout as modern combustors are operated under lean conditions to reduce emissions [13–15]. In their reviews Cavaliere et al. [16] and Marinov et al. [14] show that a significant body of work regarding lean blowout of gaseous fueled swirling flames exists. However, lean blowout of spray flames has been studied in much less detail.

Early work on spray flames was done by Lefebvre, Ballal and their co-workers and is summarized in their book [17]. Based on homogeneous fuel-air mixtures theory and balance of heat release and heat loss rates they derived a correlation to predict the equivalence ratio at lean blowout depending on combustor design, operating conditions and fuel properties [18–20]. From an analytical study of a great amount of experimental data from tests with different blends of jet fuels, Lefebvre [20] concluded that the fuel properties related to atomization and vaporization have a much stronger influence on aero-engine lean flame limits than fuel chemistry.

Lefebvre’s model was recently further developed. Hu et al. and Xie et al. [21, 22] related lean blowout to the volume of the flame instead of the volume of the combustor and Ateshkadi et al. [23] took the nozzle hardware into consideration and modified the temperature dependence term.[16] Characteristics timescales were used by Plee and Mellor [24] to describe lean blowout of bluff-body stabilized spray flames. Their model predicts lean blowout when the fuel residence time in the shear layer is less than the sum of vaporization time and reaction time. Additionally, their model

takes into account the stabilizing effects of fuel penetration to explain other experimental results that showed an "increase in the blowoff equivalence ratio with heavier fuels" [24]. An additional flame zone extending into the free stream was explained by slowly evaporating drops penetrating the bluff-body recirculation zone shear layer [25]. Although their model was initially developed for bluff body stabilized spray flames, it was successfully extended to full annular combustors with swirl-stabilized spray flames [26–28] and was also used for alternative fuel blends [29].

More recently, Marinov et al. [14] used an approach to study lean kerosene and methane flames and their lean limit in one single burner without significantly changing the hardware environment. They found strong differences in flame structure at similar flow fields and conclude that stability characteristics of spray flames cannot be satisfactorily explained by means of similarity to gaseous flames. They highlight the relevance of the liquid fuel transport and the resulting mixture fraction distribution together with vaporization time scales for spray flames. A similar approach was used by Cavaliere et al. [16] to investigate lean blowoff of premixed and non-premixed methane flames and *n*-heptane spray flames in one combustor with a bluff body swirl burner. They quantified the average blowoff times and found them to be shorter for spray flames when compared to gaseous fueled flames. They applied a correlation for premixed gaseous flames based on Damköhler number derived from Radhakrishnan et al. [30] to their flames.

The specific influence of different liquid fuels on lean blowout of swirl-stabilized spray flames has been investigated by Burger et al. [31, 32]. From their tests with a laboratory scale swirl-stabilized spray flame they concluded that lean blowout limits are potentially influenced by both physical and chemical fuel properties [31]. However, they only found minor differences in lean blowout between eight test fuels using a full annular RQL (rich quench lean) combustor under simulated altitude real engine conditions [32]. Recently, Rock et al. [33] studied fuel influence on lean blowout of swirl-stabilized spray flames using two different kind of atomizers. For a pressure atomizer their results suggest that flames which are burning fuels that are more difficult to atomize and vaporize have better lean blowout limits. For an airblast atomizer they found no strong correlation with fuel physical properties but with the fraction of branched alkanes. They also observed sensitivity of lean blowout conditions to the thermal state of the combustor.

In the next section the experimental setup of this work is described. It is followed by a presentation of the fuels that were selected for this study and an analysis of their physical and chemical properties in section IV. The measurement techniques are presented in section V and the results are shown in section VI. In the last section the results are discussed and some conclusions are drawn.

III. Experimental setup

Two co-axial, co-rotating swirling air flows were formed by a nozzle configuration consisting of an inner and an outer swirler as shown in Fig. 1(a). At the exit plane the inner swirler had an outlet diameter of $d_i = 8$ mm and the outer swirler had an outer diameter of $d_o = 11.6$ mm. The geometrical swirl numbers of this configuration were $S_c = 1.17$ for the centre flow and $S_a = 1.22$ for the annular flow. The air flows were separated by an annular ring with a sharp edge. The fuel was sprayed onto the inner surface of the ring by a pressure-swirl atomizer that produced a hollow cone spray. A liquid film was then formed which transported the fuel to the atomizer lip where it was re-atomized and injected into the combustion chamber. This airblast atomizer configuration was chosen to exhibit characteristics of aero-engine fuel injection. The combustion chamber provided almost full optical access through four quartz windows that were held by four steel posts. The cross section of the vertically arranged chamber was 85 mm by 85 mm and its height 169 mm. The burner top plate provided a round exit port for the exhaust gases with an inner diameter of 40 mm. The

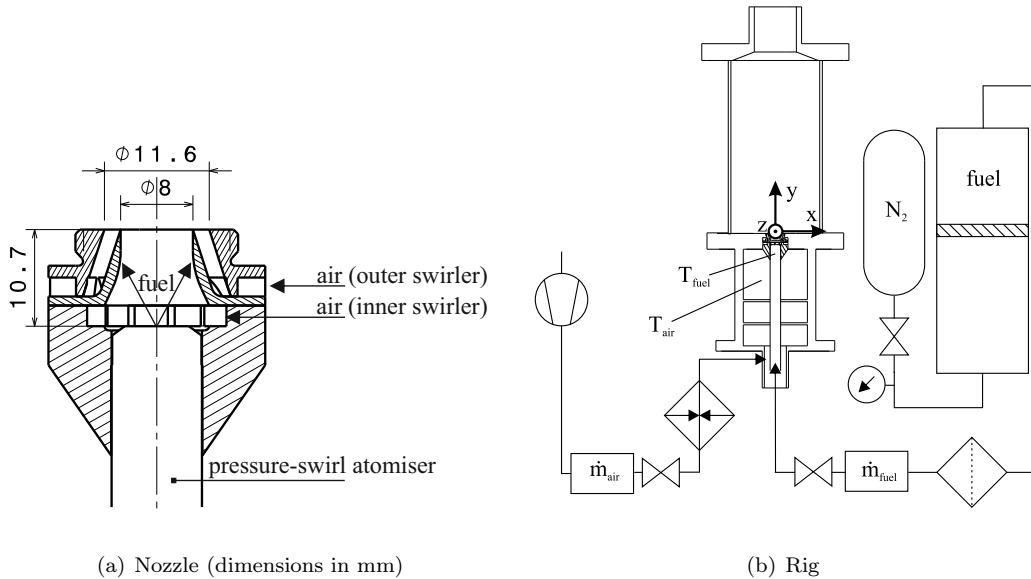


Fig. 1 Experimental setup (components not to scale) [4].

exit boundary condition was atmospheric pressure.

The combustor and peripheral devices are shown in Fig. 1(b). Dry air was supplied by a compressor and the air flow rate was controlled with a thermal mass flow controller (*Bronkhorst EL-FLOW select F-203AV*) with a stated accuracy of $\pm 0.5\%$ of reading plus $\pm 0.1\%$ of full scale. Air preheating was possible with an electrical 6 kW air heater. The burner was mounted on a three axis traverse. Fuel was pressurized in a steel cylinder and the fuel flow rate was controlled by a Coriolis type mass flow controller (*Bronkhorst mini CORI-FLOW M14*, accuracy $\pm 0.2\%$). The fuel was fed through a lance that was connected to the pressure-swirl atomizer. The lance was insulated from the plenum air by temperature controlled water flow. The fuel temperature was measured a small distance upstream of its first atomization and was kept constant for different flame and fuel cases with identical air preheat temperature. The air temperature was measured inside the plenum with a thermocouple located half way between the fuel lance and the plenum wall at a distance of 32 mm upstream of the inner swirler. More details on the combustor including the nozzle and peripheral devices can be found in a previous publication [4].

A reference flame was chosen. It was operated with a combustion air mass flow of $\dot{m}_{air} = 4.3 \text{ g/s}$ at a global equivalence ratio of $\phi = 0.8$ which resulted in a thermal power of around $P_{th} \approx 10 \text{ kW}$ depending on which fuel was used. For lean blowout measurements the air mass flow rate was varied in the range of $\dot{m}_{air} = 2.2 \text{ g/s}$ to 12.9 g/s . Photographs of flames burning the four selected fuels of this study at reference conditions are shown in Fig. 2.

To study the effect of air preheat, the temperature of the air in the plenum was varied. Two temperatures were selected: $T_{air} = 50^\circ\text{C}$ and $T_{air} = 150^\circ\text{C}$. The measured air temperatures had

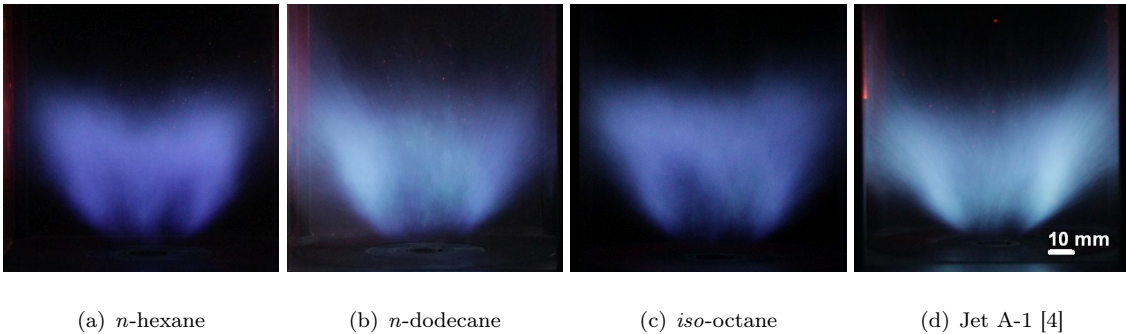


Fig. 2 Photographs of reference flames burning different fuels ($T_{air} = 50^\circ\text{C}$).

an average deviation from their nominal values of about ± 1 K. The Reynolds number of the lower air temperature reference case based on the outer outlet diameter was about $Re \approx 25000$. The fuel temperature close to the pressure swirl atomizer outlet was kept constant at $T_{fuel} = 30^\circ\text{C}$ for the lower air temperature and at $T_{fuel} = 50^\circ\text{C}$ for the higher air temperature. Due to strong heat transfer from the plenum air into the fuel lance, the fuel temperature for the higher air temperature test could not be kept at the same level as for that with the lower air temperature. However it was kept constant for variations in air mass flow rate, equivalence ratio and fuel in the respective cases. The measured fuel temperatures had an average deviation from their nominal values of about ± 1 K for the lower temperature case and about ± 5 K for the higher temperature case.

IV. Selected fuels for this study and their properties

Three single-component hydrocarbons were selected for this study: *n*-hexane, *n*-dodecane and *iso*-octane. They had a purity greater than 99 %. *n*-Hexane and *n*-dodecane represent short and long linear alkanes and *iso*-octane (2,2,4-trimethylpentane) is a representative for the branched alkanes. For comparison all measurements were also performed with kerosene Jet A-1 as a reference.

As indicated above, the global equivalence ratio and the air mass flow rate were kept constant to define reference conditions for all fuels. As a result the thermal power, the fuel mass flow rate and the adiabatic flame temperature differed between the various fuel cases. Such differences are unavoidable when comparing fuels. However, for the chosen fuels of this study, the differences are relatively small. Table 1 shows the values of these four parameters for the selected fuels at reference conditions. The equivalence ratio of the Jet A-1 was calculated based on its average C:H ratio.

	<i>n</i> -hexane	<i>n</i> -dodecane	<i>iso</i> -octane	Jet A-1
ϕ	0.8	0.8	0.8	0.8
P_{th}	10.12 kW	10.12 kW	10.10 kW	10.22 kW
\dot{m}_{fuel}	814.1 g/h	826.3 g/h	820.1 g/h	850.0 g/h
T_{ad}	2065.2 K	2069.6 K	2067.4 K	n.a.

Table 1 Flame parameters of the studied fuels at reference conditions ($\dot{m}_{air} = 4.3 \text{ g/s}$).

Some of the thermodynamic properties, e.g. the heat capacity, are usually declared per quantity of fuel. This can be achieved on a mass or a molar basis. Depending on the relative size differences

of the molecules, this can lead to different fuel rankings. However, as shown in Table 1, the fuel mass flow rates at comparable equivalence ratios are relatively close to each other. Furthermore, the comparison of lean blowout behavior is done on an equivalence ratio basis. Therefore we consider the mass specific quantities to be relevant for fuel comparisons in this study.

In the following sections we look at process relevant physical and chemical properties of the selected fuels. Most of the properties depend on temperature (and also pressure) and on its way from initial atomization to final combustion the fuel is exposed to a variety of temperatures. Hence, characteristic fuel properties need to be compared at different temperatures as their relative difference might be temperature dependent as well. As all experiments were performed at atmospheric pressure, the influence of pressure on the physical and chemical properties was not addressed. The fuel properties data were taken from the *ThermoData Engine (TDE)* [34–36], version 2.1, if not stated otherwise.

A. Atomization properties

Three physical fuel parameters are commonly known to have an impact on atomization quality of a liquid fuel: density, viscosity and surface tension. Figure 3 shows their temperature dependence for the three single-component fuels of this study for a temperature range between $T_{fuel} = 30^\circ\text{C}$ and their respective boiling point. Two main conclusions can be drawn. Firstly, the lines show no intersections at any temperature. Hence, whatever the impact of one of the parameters on atomization is, their fuel related order is independent of the temperature. This means we do not

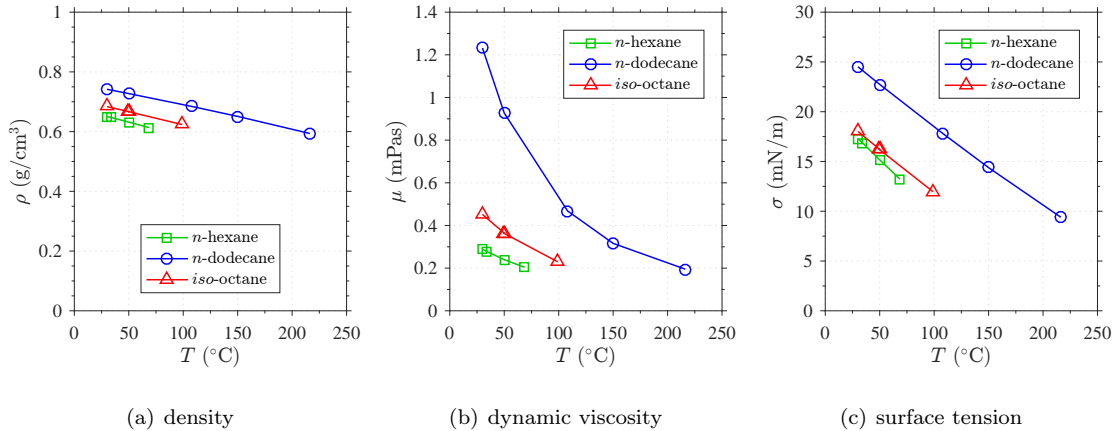


Fig. 3 Comparison of atomization properties of the studied fuels at atmospheric pressure [35].

expect one fuel to have a much different atomization performance relative to another fuel at low temperature than at high temperature. Secondly, the properties of *n*-hexane and *iso*-octane lie considerably closer to each other than to the long linear alkane *n*-dodecane. This is particularly apparent for dynamic viscosity and surface tension which are known to have a strong impact on prefilming airblast atomization, compared to liquid density which is considered to have little effect on mean drop size [37–40]. Therefore it can be concluded that the difference in atomization properties between *n*-hexane and *iso*-octane is negligible in comparison to their difference to *n*-dodecane. Furthermore *n*-hexane and *iso*-octane are expected to atomize into finer droplets than *n*-dodecane as their viscosity and surface tension are considerably lower.

B. Vaporization properties

The evaporation process is influenced by a multitude of thermodynamical properties (vapor pressure, enthalpy of vaporization, specific heat capacity, heat conductivity, to name a few) and process properties (such as pressure, temperature, relative velocity of the droplet to the gas flow, species concentration in the gas field). To gain a first understanding of the differences in the fuel evaporation behavior, the boiling points are compared. The boiling points of *n*-hexane (68.7 °C) and *iso*-octane (99.1 °C) are relatively similar and the boiling point of *n*-dodecane (216.3 °C) is twice as high.[41]

This is also reflected in the evolution of the vapor pressure with temperature as reported in Fig. 4(a). In consequence one can assume a similar evaporation behavior of *n*-hexane and *iso*-octane. In contrast, the enthalpy of vaporization does not show the same tendencies (see Fig. 4(b)). At low intermediate liquid temperatures *n*-hexane has the highest enthalpy of vaporization, which slows down the evaporation process.

To quantitatively analyse the differences in the evaporation processes the effective evaporation rate λ_{eff} as defined by Lefebvre [17]

$$\lambda_{eff} = \frac{d_0^2}{t_e} \quad (1)$$

is used. t_e is the total evaporation time (including droplet heating up) and d_0 is the initial diameter. The effective evaporation rate was also considered by Lefebvre as one of the influencing parameters

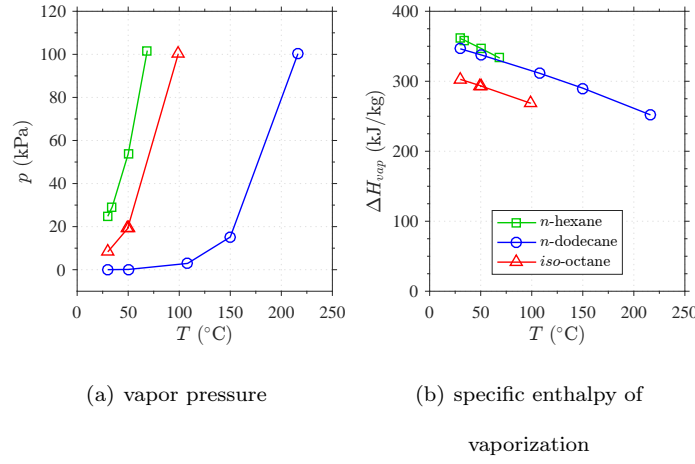


Fig. 4 Comparison of vaporization properties of the studied fuels at atmospheric pressure [35].

on lean blowout [17].

The in-house code Spraysim was used to compute the effective evaporation rates. It is a simulation tool developed at the DLR, Institute of Combustion Technology, for spray systems found in premixing/prevaporizing modules and gas turbine combustors and has been described in previous publications (e.g. by Rauch et al. [42]). The evaporation model is based on the model of Abramzon and Sirignano [43] and extended to multicomponent fuels. The high reliability and accuracy of the evaporation model was shown in several validation studies (e.g. [42]). Figure 5 shows the effective evaporation rate for all fuels in comparison. The initial air temperature was varied. One can see, that the effective evaporation rates of *n*-hexane and *iso*-octane are practically the same over the whole temperature range. This confirms the conclusion drawn based on the thermodynamic prop-

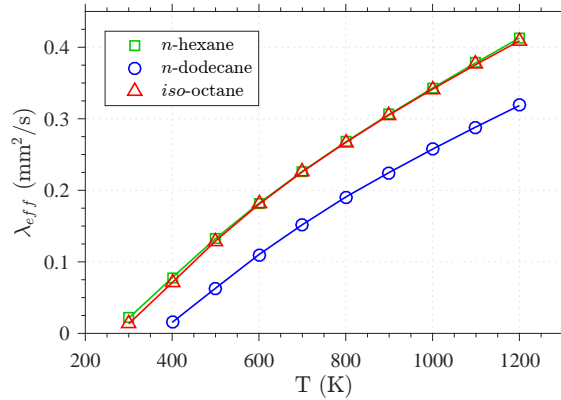


Fig. 5 Evolution of the effective evaporation rate as function of ambient gas temperature.

erties of the fuels that the difference in vaporization of *n*-hexane and *iso*-octane is small compared to their difference to *n*-dodecane. To compute the evaporation rate, the initial conditions of the droplets were the same for all fuels with an initial diameter of $d_0 = 30\text{ }\mu\text{m}$, a constant initial liquid phase temperature of $T_{liq,0} = 30^\circ\text{C}$ and an initial relative velocity between air and droplets of $v_{rel,0} = 2\text{ m/s}$. In reality these might be slightly different between fuels and depend on the type of fuel and preceding processes.

C. Chemical kinetics properties

Several characteristics are usually used to describe the chemical kinetic properties of fuels. Among those are laminar flame speed, ignition delay time and extinction strain rate. In a series of experiments Holley et al. [44–46] determined extinction strain rates of a wide range of single-component hydrocarbons and jet fuel mixtures. They found the weak extinction strain rates of *n*-heptane to exceed those of *iso*-octane for a wide range of equivalence ratios [44] and found *n*-octane flames to be more resistant to extinction than *iso*-octane flames [45]. Implications of these results for flame stability were concluded and the importance of branched alkanes on the flame response was highlighted. When comparing linear alkanes they found those with smaller carbon numbers to have greater resistance to extinction than those with longer carbon chains, which was explained by molecular mass diffusivity [46]. In a similar setup Won et al. [47] found *iso*-octane to have notably poorer extinction strain rates than a set of *n*-alkanes ranging between 7 and 10 in carbon number. When compared on a fuel mass fraction basis they also found the highest extinction resistance with the shortest *n*-alkane.

When validating a detailed chemical reaction mechanism of *n*-alkanes from *n*-octane to *n*-hexadecane, Westbrook et al. [48] found that ignition delay times at higher temperatures and species profiles of a jet stirred reactor of the *n*-alkanes are very similar. They concluded that those *n*-alkanes are sufficiently similar that they can be exchanged among each other in many application simulations. In their literature review they also mentioned that straight chain hydrocarbons are more easily ignited under (piston) engine conditions than branched hydrocarbons. The similarity in ignition delay times of higher *n*-alkanes was also confirmed by Davidson et al. [49] at temperatures above 1250 K. Li et al. [50] used shock tube measurements to determine ignition delay times of

three branched alkanes. In their literature review they list a wide range of previous studies that have found generally lower reactivity of branched alkanes compared to linear alkanes. By comparing their data to ignition delay times of linear alkanes they could confirm that an increase in the degree of carbon chain branching increases the ignition delay times.

From a review of laminar flame speed measurements and corresponding modelling Ranzi et al. [51] concluded that laminar flame speeds of linear alkanes with carbon numbers of four or more are nearly identical. Branched hydrocarbons however, have lower burning velocities than their corresponding normal component. Similar observations were made e.g. by Naik et al. [52] who found a low sensitivity to differences in fuel composition for fuels that are mainly composed of *n*-alkanes with seven or more carbon atoms.

To support the above findings from literature, two parameters, namely laminar flame speed and ignition delay times, were modelled for the above three fuels by an in-house kinetic model. Figure 6 shows the comparison of laminar flame speeds and ignition delay times of *n*-hexane, *n*-dodecane and *iso*-octane at atmospheric pressure conditions.

To predict laminar premixed flame speed and ignition delay time *Chemical WorkBench* [53] was used. The simulations of the adiabatic freely propagating flames to calculate laminar flame speeds required the initial flame conditions, i.e. fuel-oxidizer composition, temperature, and pressure. The flames were calculated considering thermal diffusion using a multi-component transport model. Ignition delay times were calculated based on a 0-D homogeneous constant volume reactor model with the initial mixture composition and the initial temperature and pressure behind the reflected shock wave as input. The temperature was calculated for adiabatic conditions and the ignition delay times were determined from the onset of temperature profiles. The reaction mechanisms for the fuels selected in this study were derived from the reaction kinetic data base under constant development at DLR [54].

Figure 6(a) shows that the flame speed of *iso*-octane is lowest compared to the two *n*-alkanes. The ignition delay times in Fig. 6(b) show that the *n*-alkanes are more reactive than *iso*-octane which shows longer ignition delay times. These properties are similar in the *n*-alkanes compared to *iso*-octane. The difference in *n*- and *iso*-alkanes flame speeds as well as ignition delay times

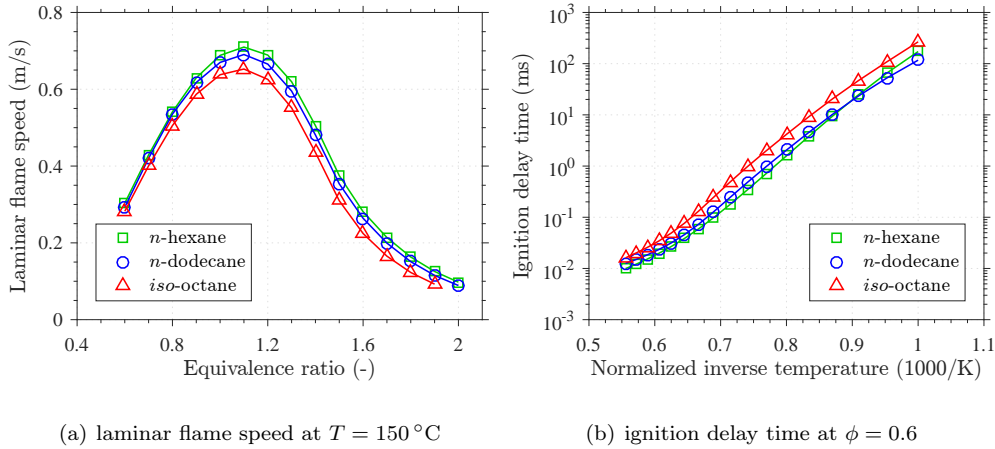


Fig. 6 Comparison of chemical kinetics properties of the selected fuels.

arise from the intermediates that are formed in the direct fuel decomposition channel. The overall reactivity of the fuel is determined not just by the first fuel radicals that are formed but rather by the type of smaller intermediates ($<C_4$) that are consequently formed and their subsequent consumption either by chain terminating or chain propagating reaction steps. As an example Ji et al. [55] showed that compared to *n*-alkanes, highly branched alkanes had larger concentrations of stable intermediates such as propene and butane which are comparatively less reactive.

We conclude that from a chemical kinetic point of view only minor differences exist in laminar flame speed and ignition delay times between linear alkanes compared to their difference to branched alkanes. Regarding extinction strain rates in prevaporized counterflow flames, short chain *n*-alkanes are considered to be more resistant to extinction than long chain *n*-alkanes and branched alkanes have a negative influence on weak extinction when compared to similar length linear alkanes.

D. Conclusion of fuel properties analysis

From the analysis of the fuel properties we draw the conclusion that two of the three selected single-component fuels, *n*-hexane and *iso*-octane, exhibit very strong similarities in atomization and vaporization properties, whilst showing significant differences in chemical kinetics properties (linear versus branched hydrocarbons). At the same time, both fuels show strong differences in vaporization and atomization properties to the third fuel, *n*-dodecane. Finally, regarding chemical kinetics, *n*-dodecane behaves similarly to *n*-hexane apart from the weak extinction performance where it is outperformed by *n*-hexane.

V. Measurement techniques

A. Lean blowout

Selecting an air mass flow rate in the range of $\dot{m}_{air} = 2.2 \text{ g/s}$ to 12.9 g/s the lean blowout limits of the fuels were determined by slowly reducing the fuel mass flow rate whilst keeping the selected air mass flow rate constant. By keeping the selected air mass flow rates constant the turbulence intensity was kept at similar levels between fuels. To begin with, the burner was thermally stabilized by operating a lean flame of $\phi = 0.6$ until the fuel and air temperatures were stable. The fuel flow rate was then reduced to approximately 80 g/h above the expected lean blowout limit. It was then slowly reduced further with a constant rate of 0.5 g/h/s , corresponding to reduction rates of ϕ in the order of 0.001 1/s to 0.0001 1/s , depending on the air mass flow rate. When the flame fully extinguished the corresponding equivalence ratio ϕ_{LBO} was recorded. This method was repeated three times per operating condition. The arithmetic averages of the three results are shown in the results section. The procedure was the same for all fuels. The absolute accuracy of the result in equivalence ratio at lean blowout was essentially determined by the accuracy of the mass flow meters (see section III). The repeatability between the three blowout events was good with an average relative deviation from the mean value at the lowest air mass flow rate of 1.2% and 0.2% at the highest air mass flow rate. The larger scatter at lower air mass flow rates was presumably due to poorer atomization at these operating conditions.

For most of the operating conditions the flame exhibited blowout pulsations before it finally blew out. In these cases the value of the equivalence ratio at the final blowout was recorded. For the remaining operating conditions combustion was stable until the flame suddenly blew out. At very low air mass flow rates and for the less volatile fuels, the discrepancy between the fuel flow rate at which the flame first became unstable and the fuel flow rate at which it finally blew out diminished. Note that lower air mass flow rates implied a lower thermal power and therefore cooler combustion chamber walls.

B. Spray characteristics

1. Mie scattering

The liquid fuel loading was determined by recording the Mie scattering signal off the fuel droplets from a 532 nm laser light sheet that was generated by a frequency doubled Nd:YAG double cavity laser (*New Wave Solo PIV*). The laser energy was attenuated to about 3 mJ/pulse to avoid camera chip saturation. The signal was recorded with a CCD camera (*LaVision Imager Intense*) with a maximum resolution of 1376×1040 pixel and a dynamic range of 12 bit. A camera objective with $f = 50$ mm (*Nikon*) was used and the aperture and exposure time were kept constant for all cases. For each case 6000 images were recorded at a rate of 5 Hz. To determine an average liquid phase loading the individual, background corrected images were binarized with a common constant threshold so that areas without droplets had a value of 0 and areas with droplets a value of 1. Then, the average of the set of images was computed. The result can be interpreted as a probability map of fuel residence (conditional liquid loading). The choice of the threshold and the amount of laser energy were expected to be the greatest sources of error regarding the absolute value of liquid loading. However, as the same settings were used for all fuels, the relative error between different fuels is expected to be small.

2. Phase Doppler Interferometry

For determination of droplet characteristics a commercial three component Phase Doppler Interferometry (PDI) system (*Artium Technologies Inc. PDI-300 MD*) was used. Axial, radial and circumferential velocity components and drop diameters of the fuel spray could be measured. Two transmitting units with three diode pumped solid state lasers were used to generate 3 pairs of laser beams: 532 nm (axial velocity and diameters), 491 nm (radial and circumferential velocity), 561 nm (radial and circumferential velocity). Respectively one of the beams of each pair was frequency shifted with a Bragg cell to allow for negative velocity measurements. The signal was collected by a receiving unit in a 45° forward scatter configuration. The focal lengths of transmitting and receiving optics were 350 mm. This resulted in a beam waist in the probe volume of approximately

150 – 180 μm depending on beam wavelength. A spatial aperture of 500 μm was applied. With this configuration droplet diameter measurements between 0.7 μm and 100 μm were possible. The refractive indices of the fuels were determined at room temperature using a refractometer and are shown in Table 2. The amplifier voltages of the signal receiving photo multipliers and their apertures were

	<i>n</i> -hexane	<i>n</i> -dodecane	<i>iso</i> -octane	Jet A-1
n	1.38	1.42	1.39	1.44

Table 2 Measured refractive indices

adjusted to the local requirements of each measurement location. By these means, saturation of the photo multipliers was minimized whilst collecting as much signal from the small droplets as possible. The combustor was traversed along x at $z = 0$ mm at two different distances from the exit plane: $y = 15$ mm and $y = 25$ mm (see coordinate system in Fig. 1(b)). At each measurement location a minimum of 5000 events that were coincident for all three channels was recorded. This lead to approximately 15000-35000 events for the first channel which was used for diameter measurements. To improve statistical quality, all valid events were used for mean diameter calculations.

VI. Results

A. Lean blowout limits

Figure 7 shows the global equivalence ratios, at which lean blowout was detected, as a function of air mass flow rate for the selected fuels at two different air preheat temperatures. Noticeable differences between the fuels are visible, particularly for the lower air temperature. At the lower air temperature, *iso*-octane has the highest values of ϕ_{LBO} and *n*-dodecane has the lowest, close to those of Jet A-1. The values of *n*-hexane lie between the two other single-component fuels, at lower air mass flow rates closer to *iso*-octane. The course of the curves is generally quite similar for all fuels: the ϕ_{LBO} values decrease slightly with decreasing air mass flow rate, before they increase again at very low air mass flow rates. The order of the fuels is independent of the operating point since the curves do not cross. However, the increase in lean blowout equivalence ratio at higher air mass flow rates is particularly pronounced with *n*-dodecane and Jet A-1.

The general course of the curves was previously explained by the competing processes of at-

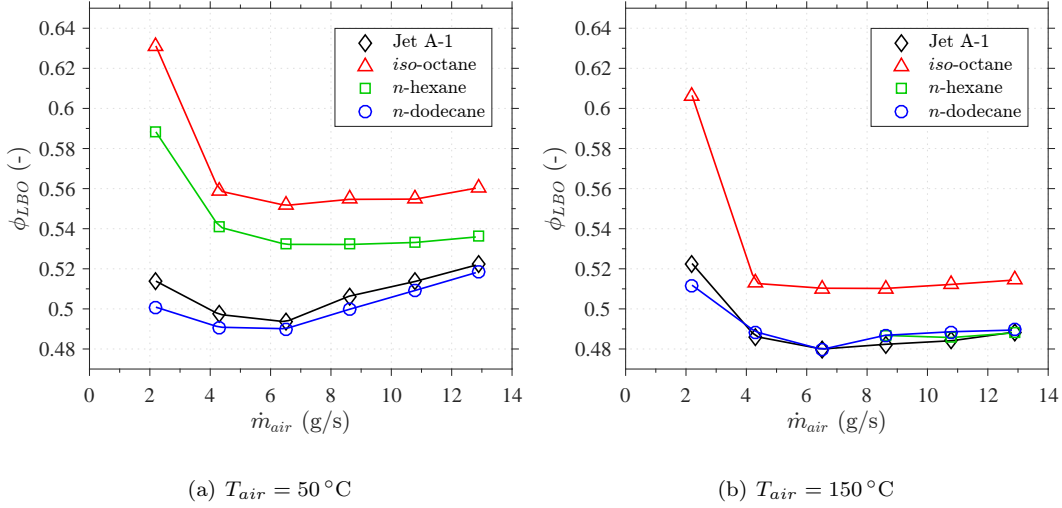


Fig. 7 Lean blowout results of the selected fuels at two air preheat temperatures.

omization, vaporization, mixing, flame chemistry and turbulence.[4] Atomization and mixing are promoted at high air flow rates but high strain rates limit the flame stabilization. At low air flow rates, strain rates decrease and the residence time is increased but the fuel atomization degrades.[4] Another possible reason for the increase in lean blowout equivalence ratio at low air mass flow rates is an increased heat transfer between the plenum air and the water cooled fuel lance. This could lead to localized reduced air temperatures that would affect especially the low boiling point fuels.

The effect of stronger preheating of the air was an overall improvement of the lean blowout limits in the range of high air mass flow rates. The fuels lie closer together, *iso*-octane still exhibits the highest values of ϕ_{LBO} , while the difference between *n*-hexane and *n*-dodecane/Jet A-1 has disappeared. At high air preheat temperature it was not possible to measure the equivalence ratio at lean blowout of *n*-hexane at low air flow rates because the fuel would have started to boil in the feed line which passed through the preheated air plenum. This is due to the very low boiling point of *n*-hexane.

We conclude that at a low air preheat temperature a difference in lean blowout was observed for two different *n*-alkanes with the longer chain showing better lean blowout behavior. At high air preheat temperature that difference disappeared. At both air temperatures *iso*-octane had worse lean blowout limits than all the other fuels. Furthermore, an increase in air temperature generally improved lean blowout for all fuels.

B. Spray characteristics

1. Conditional liquid phase loading

The conditional liquid phase loading of *n*-hexane and *n*-dodecane at reference conditions with the lower air preheat temperature is shown in Fig. 8(a). While all data has been acquired in the same setup the data shown for *n*-hexane has been mirrored at $x = 0$ mm for easier comparison. No data were processed upstream of $y \approx 15$ mm because of camera saturation due to high spray density. Values smaller than 0.5 % were set to zero. A significant difference between the two fuels is visible. The *n*-dodecane spray penetrates the combustion chamber to a height of $y \approx 55$ mm, while almost no liquid *n*-hexane fuel is found upstream of $y \approx 35$ mm. For *n*-dodecane, liquid fuel is found close to the combustor walls with a low probability of a few percent. This is not the case for *n*-hexane as it is almost fully evaporated at $|x| \approx 35$ mm. Figure 8(b) shows the liquid phase loading of *n*-hexane and *iso*-octane. The two fuels show a very similar behavior.

Smoothed horizontal profiles at a height of $y \approx 25$ mm were taken for all four fuels of this study. They are shown in Fig. 9. A strong difference between *n*-dodecane and the two lighter fuels *n*-hexane and *iso*-octane is visible. The chances to find *n*-dodecane droplets at this distance from the nozzle exit plane are approximately 3-5 times higher than for *n*-hexane or *iso*-octane. The difference between the two lighter fuels is small compared to their difference to *n*-dodecane. Hence, their atomization and vaporization are similar to those of *n*-dodecane, as described in section IV A and section IV B. Jet A-1 shows very similar liquid phase loading to *n*-dodecane. The noticeable

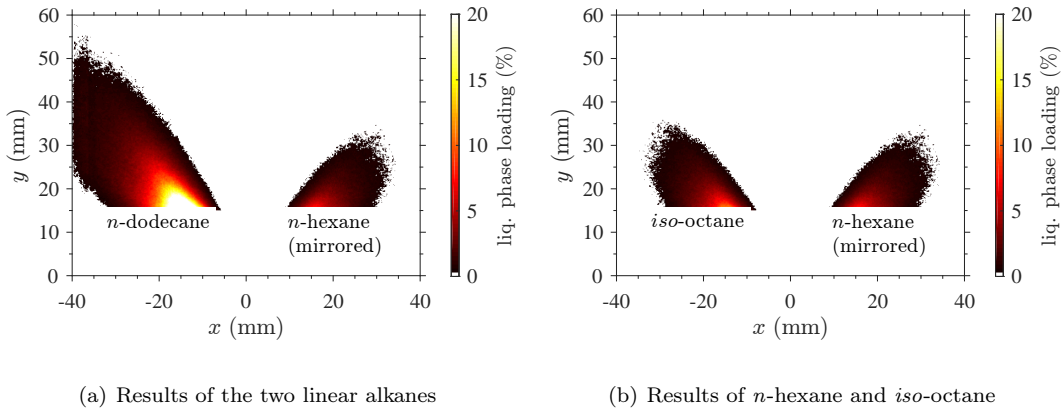


Fig. 8 Conditional liquid loading contours at the lower temperature reference case.

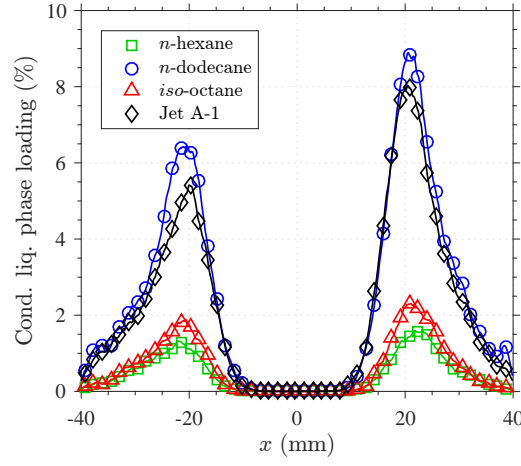


Fig. 9 Conditional liquid loading profiles at $y = 25$ mm at the lower temperature reference case.

asymmetry was described in a previous publication [4].

2. Droplet diameters

Radial Sauter mean diameter profiles for the same flame conditions are shown in Fig. 10 for two distances from the exit plane. Measurements were performed at every second millimeter on the left hand side of the combustion chamber ($x < 0$ mm). At x -positions outside the presented data the spray was too dilute and hence the average data rate was too low (< 30 Hz) to collect enough

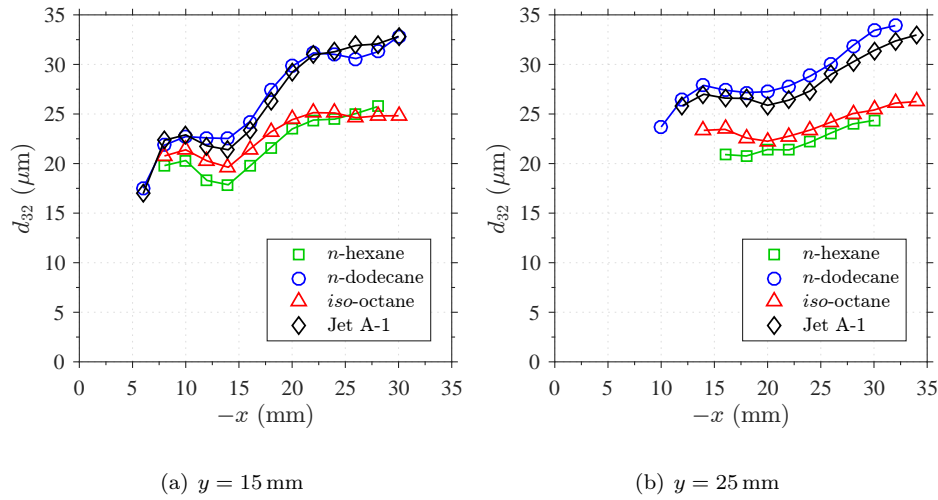


Fig. 10 Radial profiles of Sauter mean diameters at reference flame conditions ($\dot{m}_{air} = 4.3$ g/s, $\phi = 0.8$, $T_{air} = 50^\circ\text{C}$).

events in a reasonable amount of time. The Sauter mean diameter d_{32} was used as a representative diameter to transform the diameter distribution at every measurement location into a single number. Generally, it can be seen that the droplet Sauter mean diameters are within a range of $15 - 35 \mu\text{m}$. The diameters have a local minimum around the mean spray trajectory and tend to increase towards the inner and outer radial ends of the spray. This indicates that a disproportionately high number of bigger drops reach those regions of the spray. Furthermore, at the very inner radial end of the spray the Sauter mean diameter decreases again. This is due to small recirculating droplets in the inner recirculation zone. No significant differences in mean diameter can be found between the two axial distances from the exit plane, apart from in the center of the spray where the Sauter mean diameter increases further downstream. This is due to the fast vaporization of the fine droplets compared to the bigger drops. The number of the very small droplets significantly decreases and the Sauter mean diameter increases as it is more sensitive to bigger drops.

As expected from the atomization and vaporization properties, *n*-hexane and *iso*-octane show significantly smaller drops than *n*-dodecane. At the same time the difference between the two lighter fuels *n*-hexane and *iso*-octane is small compared to their common difference to *n*-dodecane. This also applies at a doubled air mass flow rate of $\dot{m}_{air} = 8.6 \text{ g/s}$, as can be seen in Fig. 11(a) and 11(b). Due to higher shear forces from the increased momentum of the air flow, the overall mean diameters decrease to $7 - 17 \mu\text{m}$ compared to the previous case. However, *n*-hexane and *iso*-octane still exhibit Sauter mean diameters very similar to each other and small compared to *n*-dodecane.

To investigate the influence of air preheating on mean droplet diameters, PDI measurements

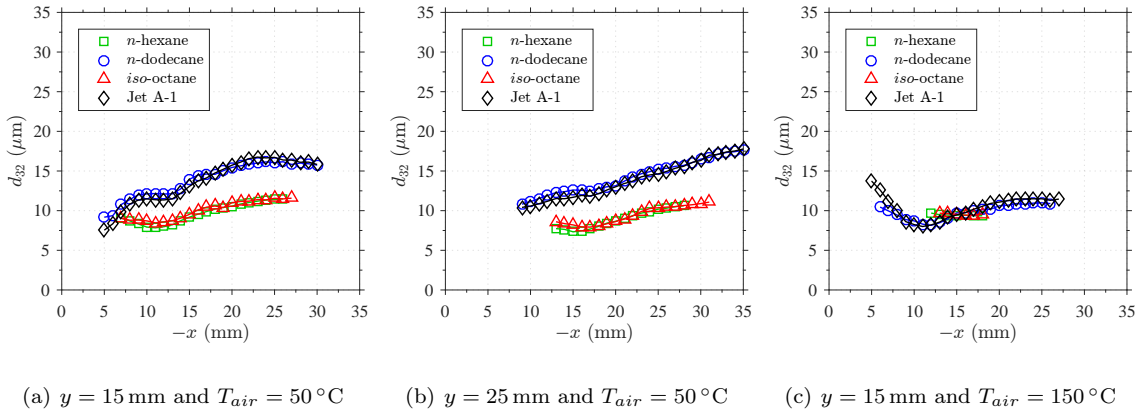


Fig. 11 Radial profiles of Sauter mean diameters at $\dot{m}_{air} = 8.6 \text{ g/s}$ and $\phi = 0.8$

were also performed at $T_{air} = 150^\circ\text{C}$ at an air mass flow rate of $\dot{m}_{air} = 8.6\text{ g/s}$. At this condition, no data could be collected at $y = 25\text{ mm}$, as too much of the fuel was already evaporated at that distance from the exit plane. The measured Sauter mean diameters at $y = 15\text{ mm}$ are shown in Fig. 11(c). Compared to $T_{air} = 50^\circ\text{C}$ (Fig. 11(a)), the size of the droplets of *n*-dodecane has decreased and now matches *n*-hexane and *iso*-octane which do not show a strong difference to the lower air preheat case. The spray of the two lighter fuels could only be measured on a radial length of approximately 7 mm, outside that length not enough liquid phase was available for data collection. These findings indicate that at the higher air preheat temperature case the sprays of *n*-hexane and *iso*-octane cover a much smaller volume than *n*-dodecane, however, where there is spray, their droplet Sauter mean diameters are relatively similar to *n*-dodecane.

Regarding the fuel mixture kerosene Jet A-1, the Sauter mean diameters were found to be very similar to those of *n*-dodecane for all cases.

VII. Discussion and conclusion

A laboratory scale combustor for swirl-stabilized, airblast atomized spray flames was used to study the lean blowout limits of three different single component hydrocarbons and kerosene Jet A-1 at atmospheric pressure conditions. The goal was to help gaining knowledge for future fuel design. The fuels' characteristics regarding atomization, vaporization and combustion chemistry were studied individually. The following general conclusions can be drawn.

A difference in lean blowout between *n*-hexane and *iso*-octane was observed at both air preheat temperatures. The branched alkane was found to be less resistant. Both fuels show very similar atomization and vaporization characteristics but differ in their chemical kinetic behavior. Therefore, the reason for the observed lean blowout difference between those fuels must be mainly of a chemical kinetic nature. This is supported by higher weak extinction strain rates of normal alkanes compared to branched alkanes [44, 45, 47] and shorter ignition delay times (cf. Fig. 6(b)). Huelskamp et al. [56] have recently shown for a dataset of bluff-body stabilized prevaporized flames that ignition delay times provide an adequate representation of the chemical time scale and correlate well with the equivalence ratio at lean blowout.

A difference in lean blowout between *n*-hexane and *n*-dodecane was observed at low air preheat

temperature. The short chain was found to be less resistant. Both fuels have very similar chemical kinetic characteristics, apart from in extinction strain rate, where short linear alkanes are considered to be more resistant to extinction than longer chains (cf. section IV C). The fuels strongly differ in their atomization and vaporization. Therefore, the chemical kinetic effect on lean blowout must be dominated by the difference in atomization and vaporization. The observed lean blowout difference at low air preheat temperature between those fuels must be mainly due to their difference in atomization and vaporization.

No difference in lean blowout between *n*-hexane and *n*-dodecane was observed at high air preheat temperature. Droplet diameter measurements indicate that the preheated air reduces the difference in atomization and vaporization. This supports the previous consideration.

It was found that a fuel that atomizes into bigger droplets and has a lower evaporation rate (*n*-dodecane), shows better lean blowout performance than a chemically similar fuel with fine spray and fast vaporizing droplets (*n*-hexane).

As mentioned above, Plee and Mellor [24] and Leonard and Mellor [25] found that slowly vaporizing droplets can have beneficial influence on lean blowout limits of spray flames. More stable combustion due to less uniform mixing was also observed by Durbin and Ballal [57], albeit using gaseous propane fuel in a swirl-stabilized combustor. The improved stability was explained by locally richer mixture regions. The same conclusion was drawn by Sturgess and Shouse [58] when comparing their lean blowout data of a swirl-stabilized generic combustor burning gaseous propane to a research combustor (well stirred reactor). Therefore, we assume that the local liquid fuel loading and the local fuel-air mixing are the main reasons for the different behavior of the two linear alkanes.

It can be concluded that fuel differences in lean blowout in this combustor can be due to differences in the physical properties as well as in the chemical properties of the fuels. Particularly the different behavior of the branched alkane shows that - at these operating conditions - chemical kinetical effects cannot be neglected in such a combustor. A correlation for lean blowout proposed by Lefebvre [20] could not be applied successfully as neither the general course of equivalence ratio at lean blowout over air mass flow rate nor the difference in local liquid fuel loading (*n*-hexane vs.

n-dodecane) were captured by the correlation.

Another aspect to consider is the influence of flame-wall interaction on flame stabilization. With respect to how the combustor was operated and how the lean blowout limit was determined, we expect the operational influence on combustion chamber wall temperatures to be similar between fuels because the same procedure was followed for each fuel. With respect to fuel influence no significant differences in thermal power existed between the fuels (see discussion of fuel properties) suggesting that the overall heat release was similar. However, different flame shapes and sizes due to different atomization and vaporization behavior and different reaction rates as discussed above could have influenced the local heat release and therefore the combustor wall temperatures. Of the three single component fuels, the slowly evaporating fuel *n*-dodecane showed particularly deep protrusion of liquid fuel in the direction of the combustor walls and hence a flame that was in contact with the combustor walls. It is unclear how this could have affected the lean blowout limits. On the one hand, the cooling effect of the combustor wall could reduce lean stability due to local quenching. On the other hand, if the wall was heated by the flame, it could have also supported flame stabilization at lean conditions. Therefore, the influence of flame-wall interaction should be investigated further, for example by measuring the flame positions at very lean conditions for the different fuels.

To continue this research it would also be valuable to investigate the lean blowout performance of the four fuels at elevated combustor pressure and higher air preheat temperature to get closer to real engine conditions. Also, prevaporization of the fuels in a combustor as similar as possible to the one of this study (dual swirl, non-premixed) would help better understanding the role of atomization and vaporization. Finally, it should be mentioned that due to the complexity of the process, probably only a numerical approach using CFD simulations of reacting flows can fully resolve the picture of liquid fuel influence on lean blowout, especially with regard to more complex fuel mixtures [59–61].

Acknowledgments

The authors would like to thank William O’Loughlin, Bhavin Kapadia and James Gounder for their support during experiments and Noël Nesanson for his support with modelling. The financial support of the Federal Ministry for Economic Affairs and Energy (Germany) within *InnoTreib* is

gratefully acknowledged. The authors are thankful for funding within the project *ECLIF* and by the Helmholtz Association within *SynKWS*.

References

- [1] Edwards, T., Moses, C., and Dryer, F., “Evaluation of Combustion Performance of Alternative Aviation Fuels,” *Proceedings of the 46th AIAA/ASME/SAE/ASEE Joint Propulsion Conference & Exhibit*, No. AIAA 2010-7155, 2010, doi:10.2514/6.2010-7155.
- [2] Braun-Unkhoff, M., Kathrotia, T., Rauch, B., and Riedel, U., “About the interaction between composition and performance of alternative jet fuels,” *CEAS Aeronautical Journal*, Vol. 7, No. 1, 2016, pp. 83–94, doi:10.1007/s13272-015-0178-8.
- [3] Blakey, S., Rye, L., and Wilson, C. W., “Aviation gas turbine alternative fuels: a review,” *Proceedings of the Combustion Institute*, Vol. 33, No. 2, 2011, pp. 2863–2885, doi:10.1016/j.proci.2010.09.011.
- [4] Grohmann, J., O’Loughlin, W., Meier, W., and Aigner, M., “Comparison of the Combustion Characteristics of Liquid Single-Component Fuels in a Gas Turbine Model Combustor,” *Proceedings of ASME Turbo Expo*, No. GT2016-56177, 2016, doi:10.1115/GT2016-56177.
- [5] Hadeif, R. and Lenze, B., “Measurements of droplets characteristics in a swirl-stabilised spray flame,” *Experimental Thermal and Fluid Science*, Vol. 30, No. 2, 2005, pp. 117–130, doi:10.1016/j.expthermflusci.2005.05.002.
- [6] Hadeif, R. and Lenze, B., “Effects of co- and counter-swirl on the droplet characteristics in a spray flame,” *Chemical Engineering and Processing*, Vol. 47, No. 12, 2008, pp. 2209–2217, doi:10.1016/j.cep.2007.11.017.
- [7] Bhagwan, R., Habisreuther, P., Zarzalis, N., and Turrini, F., “An experimental comparison of the emissions characteristics of standard Jet A-1 and synthetic fuels,” *Flow, Turbulence and Combustion*, Vol. 92, No. 4, 2014, pp. 865–884, doi:10.1007/s10494-014-9528-6.
- [8] Fokaides, P., Weiß, M., Kern, M., and Zarzalis, N., “Experimental and numerical investigation of swirl induced self-excited instabilities at the vicinity of an airblast nozzle,” *Flow, Turbulence and Combustion*, Vol. 83, No. 4, 2009, pp. 511–533, doi:10.1007/s10494-009-9205-3.
- [9] Batarseh, F. Z., Gnirß, M., Roisman, I. V., and Tropea, C., “Fluctuations of a spray generated by an airblast atomizer,” *Experiments in Fluids*, Vol. 46, No. 6, 2009, pp. 1081–1091, doi:10.1007/s00348-009-0612-y.

- [10] Zhang, C., Zou, P., Wang, B., Xue, X., Lin, Y., and Sung, C.-J., “Comparison of Flame Dynamics at Stable and Near-LBO Conditions for Swirl-Stabilized Kerosene Spray Combustion,” *Proceedings of ASME Turbo Expo*, No. GT2015-42596, 2015, doi:10.1115/GT2015-42596.
- [11] Meier, U., Heinze, J., Freitag, S., and Hassa, C., “Spray and Flame Structure of a Generic Injector at Aeroengine Conditions,” *Journal of Engineering for Gas Turbines and Power*, Vol. 134, No. 3, 2012, pp. 1–9, doi:10.1115/1.4004262.
- [12] Freitag, S., Meier, U., Heinze, J., Behrendt, T., and Hassa, C., “Measurement of initial conditions of a kerosene spray from a generic aeroengine injector at elevated pressure,” *Atomization and Sprays*, Vol. 21, No. 6, 2011, pp. 521–535, 10.1615/AtomizSpr.2011003457.
- [13] Colby, J. A., Menon, S., and Jagoda, J., “Spray and Emission Characteristics near Lean Blow Out in a Counter-Swirl Stabilized Gas Turbine Combustor,” *Proceedings of the ASME Turbo Expo*, No. GT2006-90974, 2006, doi:10.1115/GT2006-90974.
- [14] Marinov, S., Kern, M., Zarzalis, N., Habisreuther, P., Peschiulli, A., Turrini, F., and Sara, O. N., “Similarity issues of kerosene and methane confined flames stabilized by swirl in regard to the weak extinction limit,” *Flow, Turbulence and Combustion*, Vol. 89, No. 1, 2012, pp. 73–95, doi:10.1007/s10494-012-9392-1.
- [15] Bhagwan, R., Wollgarten, J. C., Habisreuther, P., and Zarzalis, N., “Experimental Investigation on Lean Blow Out of a Piloted Aeroengine Burner,” *Proceedings of ASME Turbo Expo*, No. GT2014-25199, 2014, doi:10.1115/GT2014-25199.
- [16] Cavaliere, D. E., Kariuki, J., and Mastorakos, E., “A Comparison of the Blow-Off Behaviour of Swirl-Stabilised Premixed, Non-Premixed and Spray Flames,” *Flow Turbulence Combust*, Vol. 91, No. 2, 2013, pp. 347–372, doi:10.1007/s10494-013-9470-z.
- [17] Lefebvre, A. H. and Ballal, D. R., *Gas turbine combustion: alternative fuels and emissions*, CRC Press, Taylor and Francis Group, 2010, isbn:9781420086041.
- [18] Ballal, D. R. and Lefebvre, A. H., “Weak Extinction Limits of Turbulent Flowing Mixtures,” *Journal of Engineering for Power*, Vol. 101, No. 3, 1979, pp. 343–348, doi:10.1115/1.3446582.
- [19] Ballal, D. R. and Lefebvre, A. H., “Weak Extinction Limits of Turbulent Heterogeneous Fuel/Air Mixtures,” *Journal of Engineering for Power*, Vol. 102, No. 2, 1980, pp. 416–421, doi:10.1115/79-GT-157.
- [20] Lefebvre, A. H., “Fuel Effects on gas turbine Combustion - Ignition, Stability, and Combustion Efficiency,” *Transactions of the ASME*, Vol. 107, No. 1, 1985, pp. 24–37, doi:10.1115/1.3239693.

- [21] Xie, F., Huang, Y., Hu, B., and Wang, F., “Improved Semiempirical Correlation to Predict Lean Blowout Limits for Gas Turbine Combustors,” *Journal of Propulsion and Power*, Vol. 28, No. 1, 2011, pp. 197–203, doi:10.2514/1.B34296.
- [22] Hu, B., Zhao, Q., and Xu, J., “Predicting Lean Blowout Limit of Combustors Based on Semi-Empirical Correlation and Simulation,” *Journal of Propulsion and Power*, Vol. 32, No. 1, 2016, pp. 108–120, doi:10.2514/1.B35583.
- [23] Ateshkadi, A., McDonell, V. G., and Samuelsen, G. S., “Lean blowout model for a spray-fired swirl-stabilized combustor,” *Proceedings of the Combustion Institute*, Vol. 28, No. 1, 2000, pp. 1281–1288, doi:10.1016/S0082-0784(00)80341-0.
- [24] Plee, S. L. and Mellor, A. M., “Characteristic Time Correlation for Lean Blowoff of Bluff-Body-Stabilized Flames,” *Combustion and Flame*, Vol. 35, 1979, pp. 61–80, doi:10.1016/0010-2180(79)90007-5.
- [25] Leonard, P. A. and Mellor, A. M., “Lean blowoff in high-intensity combustion with dominant fuel spray effects,” *Combustion and Flame*, Vol. 42, 1981, pp. 93–100, doi:10.1016/0010-2180(81)90144-9.
- [26] Peters, J. E. and Mellor, A. M., “Characteristic time ignition model extended to an annular gas turbine combustor,” *Journal of Energy*, Vol. 6, No. 6, 1982, pp. 439–441, doi:10.2514/3.48061.
- [27] Jarymowycz, T. A. and Mellor, A. M., “Correlation of Lean Blowoff in an Annular Combustor,” *Journal of Propulsion*, Vol. 2, No. 2, 1986, pp. 190–191, doi:10.2514/3.22866.
- [28] Derr, W. S. and Mellor, A. M., “Characteristic times for lean blowoff in turbine combustors,” *Journal of Propulsion*, Vol. 3, No. 4, 1987, pp. 377–380, doi:10.2514/3.23001.
- [29] Leonard, P. A. and Mellor, A. M., “Correlation of lean blowoff of gas turbine combustors using alternative fuels,” *Journal of Energy*, Vol. 7, No. 6, 1983, pp. 729–732, doi:10.2514/3.62722.
- [30] Radhakrishnan, K., Heywood, J., and Tabaczynski, R., “Premixed turbulent flame blowoff velocity correlation based on coherent structures in turbulent flows,” *Combustion and Flame*, Vol. 42, 1981, pp. 19–33, doi:10.1016/0010-2180(81)90139-5.
- [31] Burger, V., Yates, A., and Viljoen, C., “Influence of Fuel Physical Properties and Reaction Rate on Threshold Heterogeneous Gas Turbine Combustion,” *Proceedings of ASME Turbo Expo*, No. GT2012-68153, 2012, doi:10.1115/GT2012-68153.
- [32] Burger, V., Yates, A., Mosbach, T., and Gunasekaran, B., “Fuel Influence on targeted gas turbine Combustion properties part II: detailed results,” *Proceedings of ASME Turbo Expo*, No. GT2014-25105, 2014, doi:10.1115/GT2014-25105.
- [33] Rock, N., Chterev, I., Smith, T., Ek, H., Emerson, B., Noble, D., Seitzman, J., and Lieuwen, T., “Reacting Pressurized Spray Combustor Dynamics, Part 1. Fuel Sensitivities and Blowoff Characterization,”

- Proceedings of ASME Turbo Expo*, No. GT2016-56346, 2016, doi:10.1115/GT2016-56346.
- [34] Frenkel, M., Chirico, R., Diky, V., Yan, X., Dong, Q., and Muzny, C., “ThermoData Engine (TDE): Software Implementation of the Dynamic Data Evaluation Concept,” *Journal of Chemical Information and Modeling*, Vol. 45, No. 4, 2005, pp. 816–838, doi:10.1021/ci050067b.
 - [35] Frenkel, M., Chirico, R., Diky, V., Muzny, C., Lemmon, E. W., Yan, X., and Dong, Q., “NIST Standard Reference Database 103a, NIST ThermoData Engine, Version 2.1,” Standard Reference Data, 2005.
 - [36] Diky, V., Chirico, R., Kazakov, A. F., Muzny, C., and Frenkel, M., “ThermoData Engine (TDE): Software Implementation of the Dynamic Data Evaluation Concept. 3. Binary Mixtures,” *Journal of Chemical Information and Modeling*, Vol. 49, No. 2, 2009, pp. 503–517, doi:10.1021/ci800345e.
 - [37] Rizkalla, A. and Lefebvre, A. H., “The Influence of Air and Liquid Properties on Air Blast Atomization,” *Journal of Fluids Engineering*, Vol. 97, No. 3, 1975, pp. 316–320, doi:10.1115/1.3447309.
 - [38] Rizkalla, A. and Lefebvre, A. H., “Influence of Liquid Properties on Airblast Atomizer Spray Characteristics,” *Journal of Engineering for Power*, Vol. 97, No. 2, 1975, pp. 173–177, doi:10.1115/1.3445951.
 - [39] Lefebvre, A. H., “Airblast atomization,” *Progress in Energy and Combustion Science*, Vol. 6, No. 3, 1980, pp. 233–261, doi:10.1016/0360-1285(80)90017-9.
 - [40] Lefebvre, A. H., *Atomization and Sprays*, Hemisphere Publishing Corporation, 1989, isbn:9780891166030.
 - [41] VDI-GVC, editor, *VDI Heat Atlas*, Springer, 2nd ed., 2010, isbn:978-3-540-77876-9.
 - [42] Rauch, B., Calabria, R., Chiariello, F., Le Clercq, P., Massoli, P., and Rachner, M., “Accurate analysis of multicomponent fuel spray evaporation in turbulent flow,” *Experiments in Fluids*, Vol. 52, No. 4, 2012, pp. 935–948, doi:10.1007/s00348-011-1169-0.
 - [43] Abramzon, B. and Sirignano, W. A., “Droplet vaporization model for spray combustion calculations,” *International Journal of Heat and Mass Transfer*, Vol. 32, No. 9, 1989, pp. 1605–1618, doi:10.1016/0017-9310(89)90043-4.
 - [44] Holley, A. T., Dong, Y., Andac, M. G., and Egolfopoulos, F. N., “Extinction of premixed flames of practical liquid fuels: Experiments and simulations,” *Combustion and Flame*, Vol. 144, No. 3, 2006, pp. 448–460, doi:10.1016/j.combustflame.2005.08.001.
 - [45] Holley, A. T., Dong, Y., Andac, M. G., Egolfopoulos, F. N., and Edwards, T., “Ignition and extinction of non-premixed flames of single-component liquid hydrocarbons, jet fuels, and their surrogates,” *Proceedings of the Combustion Institute*, Vol. 31, No. 1, 2007, pp. 1205–1213, doi:10.1016/j.proci.2006.07.208.
 - [46] Holley, A. T., You, X. Q., Dames, E., Wang, H., and Egolfopoulos, F. N., “Sensitivity of propagation and extinction of large hydrocarbon flames to fuel diffusion,” *Proceedings of the Combustion Institute*,

- Vol. 32, No. 1, 2009, pp. 1157–1163, doi:10.1016/j.proci.2008.05.067.
- [47] Won, S. H., Dooley, S., Dryer, F., and Ju, Y., “A radical Index for the determination of the chemical kinetic contribution to diffusion flame extinction of large hydrocarbon fuels,” *Combustion and Flame*, Vol. 159, No. 2, 2012, pp. 541–551, doi:10.1016/j.combustflame.2011.08.020.
- [48] Westbrook, C. K., Pitz, W. J., Herbinet, O., Curran, H. J., and Silke, E. J., “A comprehensive detailed chemical kinetic reaction mechanism for combustion of n-alkane hydrocarbons from n-octane to n-hexadecane,” *Combustion and Flame*, Vol. 156, No. 1, 2009, pp. 181–199, doi:10.1016/j.combustflame.2008.07.014.
- [49] Davidson, D. F., Ranganath, S. C., Lam, K., Liaw, M., Hong, Z., and Hanson, R. K., “Ignition Delay Time Measurements of Normal Alkanes and Simple Oxygenates,” *Journal of Propulsion and Power*, Vol. 26, No. 2, 2010, pp. 280–287, doi:10.2514/1.44034.
- [50] Li, S., Campos, A., Davidson, D. F., and Hanson, R. K., “Shock tube measurements of branched alkane ignition delay times,” *Fuel*, Vol. 118, 2014, pp. 398–405, doi:10.1016/j.fuel.2013.11.028.
- [51] Ranzi, E., Frassoldati, A., Grana, R., Cuoci, A., Faravelli, T., Kelley, A. P., and Law, C. K., “Hierarchical and comparative kinetic modeling of laminar flame speeds of hydrocarbon and oxygenated fuels,” *Progress in Energy and Combustion Science*, Vol. 38, No. 4, 2012, pp. 468–501, doi:10.1016/j.pecs.2012.03.004.
- [52] Naik, C. V., Puduppakkam, K. V., Modak, A., Meeks, E., Wang, Y. L., Feng, Q., and Tsotsis, T. T., “Detailed chemical kinetic mechanism for surrogates of alternative jet fuels,” *Combustion and Flame*, Vol. 158, No. 3, 2011, pp. 434–445, doi:10.1016/j.combustflame.2010.09.016.
- [53] <http://www.kintechlab.com/products/chemical-workbench/>, “Chemical WorkBench® 4.0,” 2013.
- [54] Knyazkov, D. A., Slavinskaya, N., Dmitriev, A. G., Shmakov, A. G., Korobeinichev, O. P., and Riedel, U., “Structure of an n-heptane/toluene flame: Molecular beam mass spectrometry and computer simulation investigations,” *Combustion, Explosion, and Shock Waves*, Vol. 52, No. 2, 2016, pp. 142–154, doi:10.1134/S0010508216020039.
- [55] Ji, C., Sarathy, M., Veloo, P. S., Westbrook, C. K., and Egolfopoulos, F. N., “Effects of fuel branching on the propagation of octane isomers flames,” *Combustion and Flame*, Vol. 159, No. 4, 2012, pp. 1426–1436, doi:10.1016/j.combustflame.2011.12.004.
- [56] Huelkamp, B. C., Kiel, B. V., and Gokulakrishnan, P., “Influence of Fuel Characteristics in a Correlation to Predict Lean Blowout of Bluff-Body Stabilized Flames,” *Proceedings of ASME Turbo Expo*, No. GT2015-43433, 2015, doi:10.1115/GT2015-43433.

- [57] Durbin, M. D. and Ballal, D. R., “Studies of Lean Blowout in a Step Swirl Combustor,” *Proceedings of ASME Turbo Expo*, No. 94-GT-216, 1994, doi:10.1115/94-GT-216.
- [58] Sturgess, G. J. and Shouse, D., “Lean Blowout Research in a Generic Gas Turbine Combustor with High Optical Access,” *Proceedings of ASME Turbo Expo*, No. 93-GT-332, 1993, doi:10.1115/93-GT-332.
- [59] Asheim, J. P. and Peters, J. E., “Alternative Fuel Spray Behavior,” *Journal of Propulsion*, Vol. 5, No. 4, 1989, pp. 391–398, doi:10.2514/3.23167.
- [60] Katta, V. R. and Roquemore, W. M., “Fuel Effects on the Performance of a Recirculation-Zone Supported Burner,” *Proceedings of the 54th AIAA Aerospace Sciences Meeting*, No. AIAA 2016-0448, 2016, doi:10.2514/6.2016-0448.
- [61] Ranjan, R., Panchal, A., Hannebique, G., and Menon, S., “Towards Numerical Prediction of Jet Fuels Sensitivity of Flame Dynamics in a Swirl Spray Combustion System,” *Proceedings of the 52nd AIAA/SAE/ASEE Joint Propulsion Conference*, No. AIAA 2016-4895, 2016, doi:10.2514/6.2016-4895.